and the automatic deep learning method were 93% for the subscapularis, 90% for the supraspinatus, 84% for the infraspinatus, and 79% for the teres minor. Average Hausdorff distances between the human observers and the automatic segmentations were 0.7mm for the subscapularis, 0.3mm for the supraspinatus, 0.8mm for the infraspinatus and 0.7mm for the teres minor. Compared with the consensus of three human observers, the automatic method was able to provide goodvery good estimates of the overall muscle degeneration with a coefficient of determination (R-squared) of 0.94 for the subscapularis, 0.93 for the supraspinatus, 0.91 for the infraspinatus and 0.76 for the teres minor.

Conclusion: Deep learning-based image segmentation provides a rapid, tireless and reliable automatic quantification of RC muscle atrophy, fatty infiltration, and overall muscle degeneration in patients undergoing preoperative CT planning prior to anatomic or reverse shoulder arthroplasty, with a higher reliability and similar accuracy compared with human observers.

363 MUSCLE EDEMA OF RETRACTION AND PSEUDOFATTY INFILTRATION AFTER TRAUMATIC ROTATOR CUFF TEARS

Sidi Wang^a, Frank Kolo^b, Marko Nabergoj^c, Brigitte Von Rechenberg^d, Alexandre Lädermann^a, ^a La Tour Hospital, Geneva, Switzerland; ^bRive Droite, Geneva, Switzerland; ^cValdoltra Orthopaedic Hospital, Ankaran, Slovenia; ^dBalgrist Universitätsspital, Zurich, Switzerland

Aim: The aim of this study was 1) to confirm the existence of a new type of edema (of retraction), 2) to reveal a related potential pseudoFI, and 3) to describe the timeline of development of rotator cuff muscle edema.

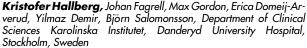
Background: Traumatic rotator's cuff's tear leads to retraction, which can be visualized on MRI. Additionally, it could also result in edematous lesions of the cuff's muscles and pseudo fatty infiltration (FI), which further evolution through time has not been described in the current literature.

Methods: We conducted in parallel two studies: a basic science study on 14 sheep to confirm the existence of muscle edema and pseudoFl, and a retrospective study of 62 prospectively identified human with a traumatic rotator cuff tear associated to muscle edema. Our cohort consisted of 49 men (79%) and 13 women (21%) with an average age of 65 years. The average time gap between the trauma and the MRI was 46 days.

Results: First, the animal study confirmed that traumatic edema of retraction exists and can be mixed up with Fl on T1 sequences. Second, we observed on human MRI that 52 patients (87%) had supraspinatus (SS) retraction; 6 (12%) had a stage 1, 25 (48%) stage 2 and 21 (40%) stage 3 retraction. Infraspinatus (IS) retraction has been observed in 33 patients (50%); 5 (15.2%) had stage 1, 16 (48.5%) stage 2 and 12 (36.4%) stage 3 retraction. Subscapularis (SSc) edema has been seen in 49 patients (79%), 30 patients (61%) had peripheral edema, 5 (10%) musculotendinous edema, 11 (22%) muscle body edema and 3 (6%) had a global SSc edema. Comparison between T1 and T2 FS/DIXON sequences of the MRI showed in 54 patients (87%) hypersignal which could be either Fl or pseudo Fl of the muscle. A positive tangent sign has been observed in only one patient (2%).

Conclusion: This study revealed a new type of edema of retraction that can appear already after few hours following a trauma. This edema has different characteristics, delay and location compared to edema of denervation. Such edema could theoretically explain muscle fibers dissections as well as rapid development of Fl observed after trauma. This edema is associated with hypersignal on Tl sequences that can be mistaken with Fl. All these findings are important regarding diagnosis, treatment and have legal implication notably to defend patients against insurances.

464 COMPUTER AIDED IDENTIFICATION AND SEVERITY GRADING OF GLENOHUMERAL OSTEOARTHRITIS AND AVASCULAR NECROSIS OF THE HUMERAL HEAD FROM PLAIN RADIOGRAPHIC IMAGES



Aim: To train a Deep learning (DL) network to identify and grade Glenohumeral osteoarthritis (GHOA) using the modified Samilson-Prieto classification system according to Allain (SPA) in plain radiographs. Our secondary aim was identical for vascular necrosis of the humeral head (AVN) using the Cruess classification system.

Background: Glenohumeral osteoarthritis and AVN are two debilitating diseases of the shoulder. Patients with any of these diseases benefit from early and correct diagnosis. DL networks, a field within artificial intelligence (AI) have in recent years shown great potential to analyse radiographic images and could potentially be trained to identify and grade GHOA and AVN in order to ensure that these diagnoses are not missed.

Methods: 6733 plain radiographic examinations were split into a training- (6172 exams) and a validation set (560 exams), for training, validation and evaluation of network performance. A DL network was trained to in turn identify and classify alone. Our primary outcome measurement was Area under curve (AUC) in Receiver Operator Characteristics (ROC) analysis.

Results: For GHOA, our network achieved an AUC ranging from 0.75 to 0.96 for individual SPA grades. SPA grade definitive and severe yielded overall best results whereas none, mild and moderate were more challenging to identify and grade. Our network achieved AUC 0.85 (95% confidence interval (CI), 0.70 to 0.99) for diagnosing AVN despite few cases in the study sample.

Conclusion: We demonstrated as a novelty, that a DL network is a feasible approach for identification and grading of GHOA and AVN on plain radiographs.

447 THE ROLE OF THE ACROMIOCLAVICULAR AND CORACOCLAVICULAR LIGAMENTS IN SHOULDER MOTION USING A THREE-DIMENSIONAL FINITE ELEMENT MODEL

Ausberto Rafael Velasquez Garcia^a, Farid Salamé Castillo^b, Joaquin Mura Mardones^b, Max Ekdahl Giordani^c, ^a Clínica Universidad de los Andes, Santiago, Chile; ^b Universidad Técnica Federico Santa María, Santiago, Chile; ^c Clínica Las Condes, Santiago, Chile

Aim: The aim was to develop a three-dimensional (3D) finite element model (FEM) of the acromioclavicular (AC) joint, which can be used in the future for the dynamic study of reconstruction techniques. The secondary objectives were to analyze stress distribution, strain, geometric and length change in the coracoclavicular (CC) and AC ligaments and to determine spatial relationships of the AC during shoulder motion.

Background: Most biomechanical studies of the AC joint analyze the function of the CC and AC ligaments based on results after their own sequential sections and extra-articular loading to the bones in the horizontal or vertical planes. These semi-rigid models keep at least one of the bones of the shoulder girdle fixed, reproducing an unreal kinematic condition. There are no reports evaluating stress as a predictor of a dynamic failure of all these ligaments during the 3D shoulder motion.

Methods: Computed tomography images of a healthy right shoulder were reconstructed and segmented. A computer aids design model was created. The ligaments were virtually reconstructed through their insertion footprints. A FEM was modeled in ANSYS 19R2 software assuming homogeneous, isotropic and hyper-elastic components. Axis alignment was identified from a 3D coordinate system. The kinematics of the shoulder girdle was recorded in both coronal plane abduction and in horizontal adduction during $10\underline{o}$ intervals of humerus motion. Von Mises equivalent stress distribution was calculated as a predictor of failure. Variations in ligaments lengths, spatial relationships of the AC joint during both movements were measured. Values p<0.05 were considered significant.

Results: The mean stress of the conoid ligament during shoulder abduction was greater than that of the trapezoid ligament (p<0.001). The maximum value (13.654 MPa) was observed at 120 $_{\rm D}$. During horizontal adduction, the highest average stress distribution (0.971 MPa) was observed in the antero-inferior AC ligament, with a maximum value of 2.174 MPa at 90 $_{\rm D}$. The lengths of the conoid ligament gradually increased between 60° and 120° of shoulder abduction (p<0.05) while those of the trapezoid and AC ligaments remained relatively consistent.

Conclusion: A simplified model was designed to effectively analyze the function of the AC and CC ligaments. The conoid is critical for preserving native kinematics in both shoulder movements. Increased stress on the antero-inferior AC ligament suggests that it is crucial for maintaining normal scapular protraction during the shoulder adduction. Their complementary mode of action suggests that both structures should be reconstructed at surgery to maintain normal AC kinematics.

395 FOUR YEARS OF CLINICAL EXPERIENCE WITH AN EVIDENCE-BASED TREATMENT ALGORITHM FOR PROXIMAL HUMERUS FRACTURES – A PROSPECTIVE COMPARATIVE STUDY



Aim: To evaluate the overall results and complications of treatment of proximal humerus fractures (PHF) using a patient-specific, evidence-based algorithm with a focus on the refinements made on the initial treatment algorithm.

Background: Operative treatment for PHF has been questioned, since randomized controlled trials could not find any functional differences between operative and nonoperative treatment. Although these studies provide high evidence, they often result in fragmented knowledge irrespective of fracture type or patient-specific factors. Therefore, an evidence-based treatment algorithm that prioritizes patients age, demands and biology was created and further refined.

Methods: Between 2014 and 2017, skeletally mature patients with isolated PHF were included and prospectively followed. The initial treatment algorithm (V1) based on patient's functional demands, bone quality and fracture type, was refined after 2 years (V2) to expand nonoperative treatment and reversed total shoulder arthroplasty (RTSA) options. Adherence to protocol, clinical outcome and complications were analyzed at 1-year postoperative.

Results: Of the 334 patients included (mean age 66 years, 68% female), 226 were treated nonoperatively, 60 with open reduction internal fixation (ORIF), 39 with RTSA and 4 with hemiarthroplasty. At 1 year, the pre-injury EQ-5D was regained (0.88 vs 0.89, p = 0.802) and the respective mean relative Constant Score (rCS) and mean Subjective Shoulder Values (SSV) were 96% and 85%. Overall complication and revision rates were 19% and 13%, respectively. A tendency toward better adherence (89% vs 83%, p = 0.060), with similar complication (16.7% vs 15.8%, p = 0.828) and revision rates (8.4%

vs 12.9%, p = 0.226) were found when comparing V2 with V1. Treatment conform the algorithm outperformed non-conforming treatment regarding rCS (97% vs 88%, p = 0.016), complication rate (16.3% vs 30.7%, p = 0.014) and revision rate (10.6% vs 26.2%, p = 0.001).

Conclusion: A patient-specific, evidence-based treatment of PHF restored pre-injury quality of life as measured by EQ-5D and approximated 90% of a normal shoulder as measured by rCS and SSV. The findings highlight that an individualized treatment of PHF is important, given that treatment conform protocol outperformed a non-conforming treatment pathway. A tendency toward better adherence while maintaining clinical outcomes was seen when expanding the nonoperative and RTSA treatment options (V2).

97 RELIABILITY OF MORPHOLOGICAL MUTCH CLASSIFICATION FOR GREATER TUBEROSITY FRACTURES OF THE PROXIMAL HUMERUS: COMPARISON OF X-RAY, TWO-, AND THREE-DIMENSIONAL CT

Sam Razaeian^a, Said Askittou^a, Dafang Zhang^b, Afif Harb^a, Christian Krettek^a, Nael Hawi^a, ^aHannover Medical School, Hannover, Germany; ^bBrigham and Women's Hospital, Boston, United States

Aim: This study aims to investigate inter- and intraobserver reliability of the morphological Mutch classification for consecutive proximal humerus fractures (PHF) with greater tuberosity (GT) involvement for three different imaging modalities (plain radiographs, two-dimensional [2-D] computed tomography [CT], and reformatted, three dimensional [3-D] CT reconstruction).

Background: The morphological Mutch classification is a simple and reliable classification for greater tuberosity (GT) fractures. However, so far, assessments of its reliability are limited to radiographic evaluations of isolated GT fractures. Recently, a potential application of this classification system to PHF with GT involvement in general has been discussed, but to date, a reliability analysis for this fracture entity has not been performed.

Methods: Óne hundred thirty-eight consecutive PHF with GT involvement were identified between January 2018 and December 2018 in a supraregional Level 1 trauma center. GT morphology was classified by three blinded observers according to the morphological Mutch classification using the picture archiving and communication software Visage 7.1 (Visage Imaging Inc., San Diego, CA, USA). Fleiss' and Cohens' kappa were assessed for inter- and intraobserver reliability. Strength of agreement for kappa (k) values was interpreted according to the Landis and Koch benchmark scale.

Results: In cases of isolated GT fractures (n=24), the morphological Mutch classification achieved consistently substantial values for interobserver reliability (radiograph: k=0.63; 2-D CT: k=0.75; 3-D CT: k=0.77). Moreover, use of advanced imaging (2-D and 3-D CT) tends to increase reliability. Consistently substantial mean values were found for intraobserver agreement (radiograph: Ø k=0.72; 2-D CT: Ø k=0.8; 3-D CT: Ø k=0.76). In cases of multi-part PHF with GT involvement (n=114), interobserver agreement was only slight to fair regardless of imaging modality (radiograph: k=0.3; 2-D CT: k=0.17; 3-D CT: k=0.05). Intraobserver agreement achieved fair to moderate mean values (radiograph: Ø k=0.56; 2-D CT: Ø k=0.61; 3-D CT: Ø k=0.33).

Conclusion: The morphological Mutch classification is a reliable classification for isolated GT fractures, particularly with 2-D or 3-D CT imaging. Usage of these advanced imaging modalities tends to increase interobserver reliability. However, its reliability for multi-part fractures with GT involvement is limited. A simple and reliable classification is missing for this fracture entity.